Pharmacogenomics and Personalized Medicine

Dovepress

open access to scientific and medical research

Open Access Full Text Article

ORIGINAL RESEARCH

Hsa_circ_0003489 Drives PTX Resistance of Human NSCLC Cells Through Modulating miR-98-5p/IGF2

Shaofeng Xia[1], Chenliang Wang[2]

[1]Department of Thoracic Surgery, The First People's Hospital of Jiujiang City, Jiujiang, Jiangxi, People's Republic of China; [2]Department of Pathology, The First People's Hospital of Jiujiang City, Jiujiang, Jiangxi, People's Republic of China

Correspondence: Chenliang Wang, Department of Pathology, The First People's Hospital of Jiujiang City, Jiujiang, Jiangxi, 332000, People's Republic of China, Tel +86–13970298684, Email wangchenliang684@126.com

Background: Circular RNAs (circRNAs) demonstrated critical roles within developing tumors and treatment resistance in an increasing body of research. The aim was to look into the functions and processes of hsa_circ_0003489 in the non-small cell lung cancer (NSCLC) paclitaxel (PTX) resistance.

Methods: NSCLC cell-based cultures including A549 and H460 were employed for such an investigation. hsa_circ_0003489, miR-98-5p, and insulin-like growth factor 2 (IGF2) expression-profiles were evaluated with a quantitative real-time polymerase chain reaction (RT-qPCR). The PTX resistance was determined using MTT assay, and the ELISA test measured IGF2 expression. Facilitating corroboration for miR-98-5p relation and hsa_circ_0003489 or IGF2, a dual-luciferase reporter method was applied.

Results: The hsa_circ_0003489 level was raised in cells and tissues from PTX-resistant (PR) NSCLC. In PR NSCLC cells, hsa_circ_0003489 knockdown reduced PTX resistance. For the purpose of the mechanism study, hsa_circ_0003489 knockdown substantially reduced IGF2 expression via miR-98-5p sponging, improving PTX sensitivity in PR NSCLC.

Conclusion: Through miR-98-5p/IGF2 axis control, hsa_circ_0003489 knockdown helped NSCLC overcome PTX resistance, suggesting a potential circRNA-targeted therapy for the disease.

Keywords: Hsa_circ_0003489, PTX resistance, NSCLC, miR-98-5p, IGF2

Introduction

Lung cancer's high frequency and mortality make it the most lethal form of the disease, killing more men and women than any other kind of cancer combined.[1] About 85% of lung cancers are NSCLC. Presently, individuals with advanced NSCLC are often treated with platinum-based combination chemotherapy.[2] The most often used first-line chemotherapy regimen for the treatment of NSCLC is cisplatin plus one of the new drugs. However, there is considerable variation in how well people respond to medication treatment, and the development of drug resistance severely constrains the possibility of a permanent cure. This is why it is crucial to determine the molecular pathways contributing to cisplatin chemoresistance in lung cancer.

Recent breakthroughs in circRNAs research indicate that circRNAs exercise their biological activities by acting as RNA sponges that bind to microRNAs (miRNAs) competitively, thereby regulating gene expression.[3–5] For instance, in NSCLC, the circ-CPA4/let-7 miRNA/PD-L1 axis controls proliferation, stemness, immune evasion, together with therapeutic resistance.[6] CircRNA_101237 through miRNA-490-3p/MAPK1 axis,[7] and hsa_circ_0041268 by sponging miR-214-5p/ROCK1 promotes NSCLC progression.[8] Several studies have shown that inhibiting circ_0014130, which regulates the miR-545-3p-YAP1 axis, may reduce drug resistance and various malignant behaviors in NSCLC cells that have acquired docetaxel resistance.[9] CircSNX6 enhances NSCLC drug resistance via miR-137.[10] Circ-CUL2/microRNA-888-5p/RB1CC1 axis contributes to NSCLC cisplatin chemoresistance.[11] Furthermore, circRNAs have been shown to

Received: 8 April 2023
Accepted: 11 August 2023
Published: 4 September 2023

have a major role in tumor growth, spread, and drug response in lung cancer; as a result, they are regarded as crucial biomarkers for the diagnosis, prognosis, and therapy of this disease.[12,13] Additionally, overexpression of IGF2 occurs in many cancers and is associated with a poor prognosis.[14] Elevated IGF2 is also associated with increased risk of developing various cancers including colorectal,[15] breast,[16] prostate[17] and lung.[18] The hsa_circ_0003489 has been identified as a new oncogene in cancer;[19] its role in cell growth and chemoresistance of NSCLC remains to be annotated.

We looked into hsa_circ_0003489 and miR-98-5p in PR NSCLC cells, hoping to learn more about their expression and function in these cells. Chemoresistance and tumor development in vivo were evaluated functionally. hsa_circ_0003489 has been reported to interact with miR-98-5p, which subsequently targets IGF2. According to our findings, hsa_circ_0003489, miR-98-5p, and IGF2 might represent prospective therapeutic targets for PTX-resistant NSCLC.

Materials and Methods

Tissues Acquisition

At Jiujiang's First People's Hospital, 146 NSCLC tissue samples were taken from patients with written informed consent. This study was formulated according to the Declaration of Helsinki. Table 1 shows correlations between hsa_circ_0003489 levels and NSCLC patient clinicopathological features. According to the Response Evaluation Criteria in Solid Tumors (RECIST), 146 samples of NSCLC were divided into the treatment sensitive group (n = 82) and the treatment resistant group (n = 64). PTX-sensitive tumors were defined as those tumors in which a ≥30% reduction was observed for the largest lesion, while PTX-resistant tumors were those without any significant change following treatment with PTX. Until usage, the samples were kept at −80 °C. The First People's Hospital of Jiujiang's Ethics Committee approved the project.

Table 1 Correlations Between Hsa_circ_0003489 Levels and NSCLC Patient Clinicopathological Features

Variable	Low hsa_circ_0003489 Expression	High hsa_circ_0003489 Expression	P value
Age (Years)			0.219
≤ 60	35	41	
> 60	38	32	
Gender			0.341
Male	55	55	
Female	18	18	
Tumor size (cm)			< 0.05
≤ 3	49	16	
> 3	24	57	
Tumor type			0.294
Squamous cell carcinoma	47	41	
Adenocarcinoma	26	32	
TNM stages			< 0.05
I–II	53	18	
III–IV	20	55	

(*Continued*)

Table 1 (Continued).

Variable	Low hsa_circ_0003489 Expression	High hsa_circ_0003489 Expression	P value
Distant metastasis or recurrence			< 0.05
Negative	54	24	
Positive	19	49	
Lymph nodes metastasis			< 0.05
Negative	49	23	
Positive	24	50	

Cell Culture

H460, A549, and primary human bronchial epithelial cells (HBE) were procured through Procell (China). H460 and A549 NSCLC cells that are resistant to PTX were created by subjecting the parent cells to higher dosages of PTX (SP8020; Solarbio, Beijing, China). Overnight cultivation of the cells was done overnight (37 °C/5% CO_2) within 1% pen-strep (Invitrogen) and 10% fetal bovine serum (FBS) supplemented RPMI1640 media (Invitrogen, USA). Additionally, media was added with 5 nM PTX (Solarbio) to keep the H460/PTX and A549/PTX cultures resistant.

Cell Transfection

IGF2 overexpression vector (IGF2), empty pcDNA, si-NC, hsa_circ_0003489 small interfering RNA, miR-98-5p mimics (miR-98-5p), miR-NC, miR-98-5p inhibitors (anti-miR-98-5p), and anti-miR-NC were all created. Following a 24-hour plating period, Lipofectamine 2000 (Invitrogen) was used for transfecting the H460/PTX and A549/PTX cells (2×10^4 cells/well within a 6-well plate) with the vectors (2 μg) or appropriate synthetic oligonucleotides (50 nM) per the manufacturer's instructions. SiRNA specifically targeting hsa_circ_0003489 is si-circ1: 5'-TCTGATAGTAAGTCTTCG -3'. The miR-98-5p mimics and miR-98-5p inhibitors purchased from MedChemExpress Ltd. (China). IGF2 overexpression vector (IGF2) and empty pcDNA purchased from HedgehogBio Science and Technology Ltd. (China).

Quantitative Real-Time Polymerase Chain Reaction (RT-qPCR)

The RNeasy Mini kit (Qiagen, USA) enabled total RNA isolation, and the NanoDrop 2000c platform (Thermo Fisher Scientific, USA) was used to measure it. Then, cDNAs were produced using either the TaqMan MicroRNA Reverse Transcription Kit (Applied Biosystem, USA) or the M-MLV Reverse Transcriptase Kit (Promega, USA). The StepOnePlus Real-Time PCR platform (Applied Biosystems) consequently manipulated RT-qPCR reaction using specific primers (RIBOBIO, China) and SYBR Green PCR Master Mix (Invitrogen, USA).

3-(4,5-Dimethylthiazol-2-yl)-2,5-Diphenyltetrazolium Bromide (MTT) Assessment

H460/PTX together with A549/PTX were seeded (5000 cells per well) in 96-well plates after siRNA/plasmid transfection, and they were then subjected to DDP, DTX, and PTX for 48 hours. Then, cells were exposed to MTT reagent (2 mg/mL, Sigma-Aldrich) and let for 4 hours to react. Resultantly, the formed formazan crystals were subjected to dissolution in dimethylsulfoxide (100 μL) followed by recording absorbance (570 nm). GraphPad Prism 7 (GraphPad Software, USA) determined IC_{50}.

Dual-Luciferase Reporter (DLR) Assay

The DLR plasmids hsa_circ_0003489-WT and IGF2-WT were created by cloning MiR-98-5p docking sites carrying hsa_circ_0003489 or IGF2 into psiCHECK2 (Promega, Fitchburg, WI). We also created the mutated plasmids

(hsa_circ_0003489-MUT and IGF2-MUT) for the aforementioned luciferase reporter plasmids. The aforementioned vector was then co-incorporated into 293T in tandem with miR-98-5p or miR-NC, and the cells were then treated (48 hours). The DLR Assay Kit was used to measure the luciferase activity (Promega).

RNA Immunoprecipitation (RIP) Assay

Millipore's EZ-Magna RIP RNA-Binding Protein Immunoprecipitation Kit (USA) was used for the RIP assessment. H460/PTX and A549/PTX cells were lysed using RIP lysis buffer and RNase I (Millipore), and 100 μL of the lysate were then treated with RIP buffer containing magnetic beads that had been coated with antibodies. Has_circ_0003489 and miR-98-5p levels were then quantified using qRT-PCR after being precipitated per the kit's instructions.

ELISA Assay

An ELISA kit (R&D Systems) was utilized for quantifying IGF2 present in the various culture media per the manufacturer's instructionsAssays were performed in triplicate runs, with dataset outcomes analyzed and published based on the average.

Statistical Analysis

Triplicates of each experiment were run. Data reflected mean ± standard deviation (SD). Variations were examined through Student's *t*-test/one-way analysis of variance (ANOVA). Spearman correlation coefficient analysis determined relationship/s across miR-98-5p and either hsa_circ_0003489 or IGF2. $P < 0.05$ was assumed to confer statistical significance.

Results

Expression-Profiling for Hsa_circ_0003489 Within PR NSCLC

The hsa_circ_0003489 expression level in PR and PTX-sensitive (PS) NSCLC tissues was first assessed using a qRT-PCR assay. Consequently, there was an apparent upward increase in the hsa_circ_0003489 expression level from PS to PR NSCLC tissue (Figure 1A). Furthermore, this investigation discovered that the amount of the hsa_circ_0003489 was higher in H460 and A549 cells than it was within HBE cultures, whilst concomitantly being downregulated in comparison to H460/PTX and A549/PTX cultures (Figure 1B). By having higher IC_{50} values from MTT assay for PTX in H460/PTX and A549/PTX, our findings indicated that PTX resistance was created in these cells (Figure 1C). In addition, resistance to digestion with RNase R exonuclease specifically degraded linear RNAs but not circRNAs (Figure 1D). The results of actinomycin D assays revealed that the half-life of the hsa_circ_0003489 transcript exceeded 24 h, longer than the 4-h half-life of CDK8 mRNA, indicating that hsa_circ_0003489 is more stable than the linear CDK8 transcript (Figure 1E).

Suppression of PTX Resistance by Hsa_circ_0003489 Knockdown in PTX-Resistant NSCLC Cells

Loss-of-function assays were performed through si-hsa_circ_0003489 transfection within H460/PTX and A549/PTX cells to inhibit the hsa_circ_0003489 expression. These experiments aimed to corroborate the roles of hsa_circ_0003489 in the PR of NSCLC. In comparison to si-NC groups, the qRT-PCR test demonstrated that si-hsa_circ_0003489 transfection resulted in a striking drop in hsa_circ_0003489 expression (Figure 2A). MTT test results demonstrated that IC_{50} of PTX was lowered, indicating hsa_circ_0003489 knockdown to suppress H460/PTX and A549/PTX chemoresistance against PTX (Figure 2B).

Hsa_circ_0003489 Sponges miR-98-5p

Following starbase 3.0 assessment, hsa_circ_0003489 was elucidated for targeting miR-98-5p, together with possible binding-locations. MiR-98-5p's sequence was found to be homologous to hsa_circ_0003489 (Figure 3A). We performed a DLR test to support the hsa_circ_0003489-miR-98-5p connection further. According to our findings, miR-98-5p

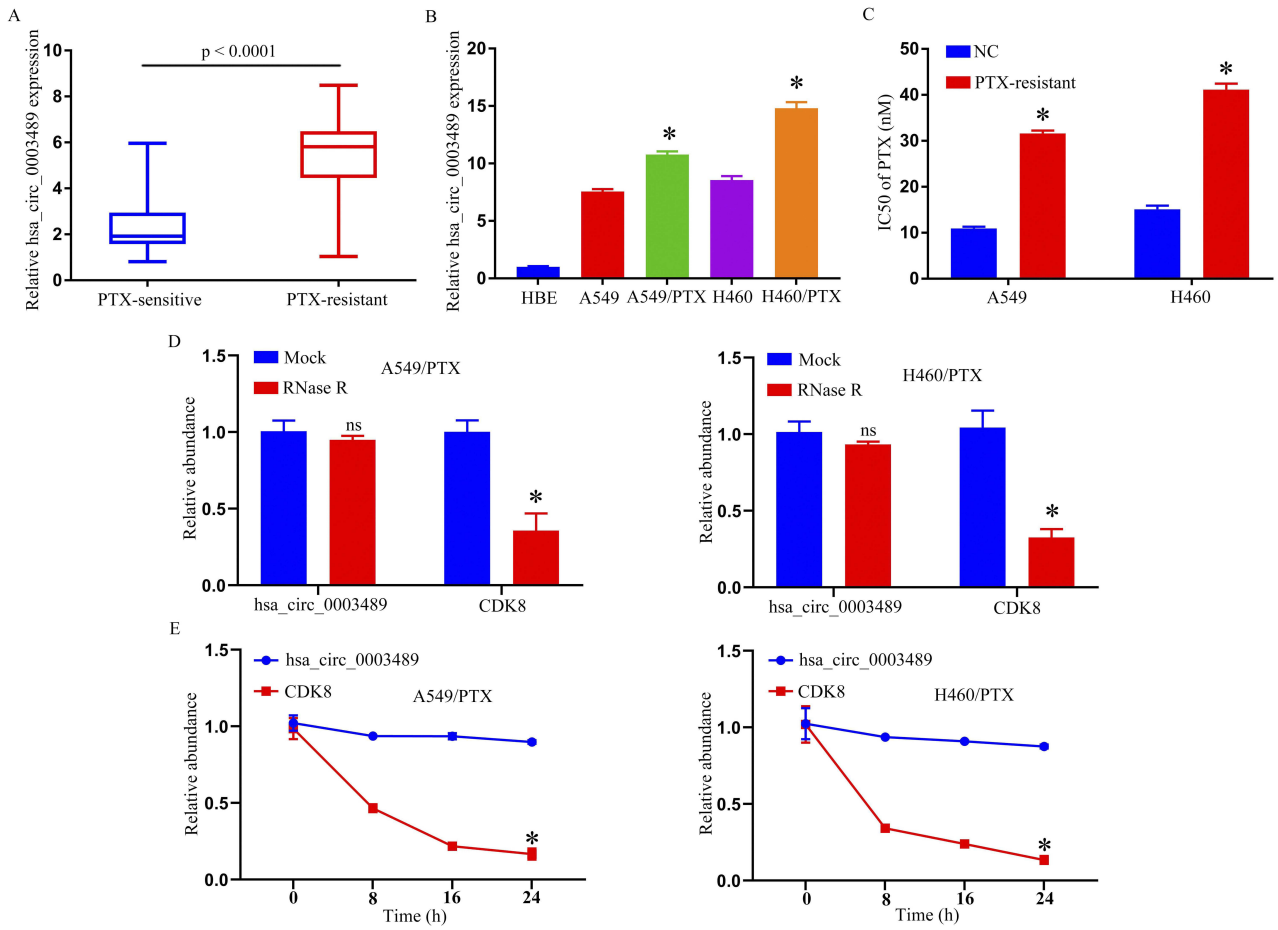

Figure 1 Expression of hsa_circ_0003489 in PTX-resistant NSCLC tissues and cell lines. (**A**) The expression of hsa_circ_0003489 in PTX-sensitive and PTX-resistant NSCLC tissues; qRT-PCR assay. (**B**) The expression of hsa_circ_0003489 in HBE, A549, H460, A549/PTX, and H460/PTX cells; qRT-PCR assay. (**C**) IC50 of PTX in A549/PTX and H460/PTX cells; MTT assay. (**D**) The expression of hsa_circ_0003489 and CDK8 mRNA after treatment with RNase R in A549/PTX and H460/PTX cells; qRT-PCR assay. (**E**) The expression of hsa_circ_0003489 and CDK8 mRNA after treatment with Actinomycin D at the indicated time points in A549/PTX and H460/PTX cells; qRT-PCR assay. *p < 0.05.

substantially lessened hsa_circ_0003489-WT luciferase gene function (Figure 3B). The hsa_circ_0003489/miR-98-5p genes were also obviously enriched in the Ago2 group when compared to lgG group, according to RIP analysis (Figure 3C). Additionally, compared to H460 and A549 cells, miR-98-5p levels within H460/PTX and A549/PTX were considerably lower (Figure 3D). Depletion of hsa_circ_0003489 also increased miR-98-5p levels (Figure 3E). Additionally, miR-98-5p levels in PR tissues were significantly lower than in their sensitive counterparts (Figure 3F). Furthermore, the miR-98-5p levels were inversely linked to hsa_circ_0003489 expression (Figure 3G). They showed a significant decrease in miR-98-5p expression upon introducing anti-miR-98-5p (Figure 3H). Finally, we showed that hsa_circ_0003489 silencing decreased cell growth (Figure 3I) and the IC50 values for PTX (Figure 3J), but anti-miR-98-5p insertion within H460/PTX and A549/PTX cells recovered such low IC_{50} values. This result was consistent with previous studies, miR-98-5p inhibited gastric cancer cell stemness and chemoresistance by targeting branched-chain aminotransferases 1.[20] By explicitly targeting miR-98-5p, hsa_circ_0003489 – overall – negatively impacted miR-98-5p expression.

IGF2 – A Direct-Downstream Target for miR-98-5p

Following starbase 3.0 assessment, miR-98-5p was elucidated for targeting IGF2, together with possible binding-locations (Figure 4A). Consequently, DLR assays verified the connection between miR-98-5p and IGF2. The findings demonstrated that, in contrast to miR-NC and IGF2-WT co-transfected cohorts, luciferase activity was thwarted within

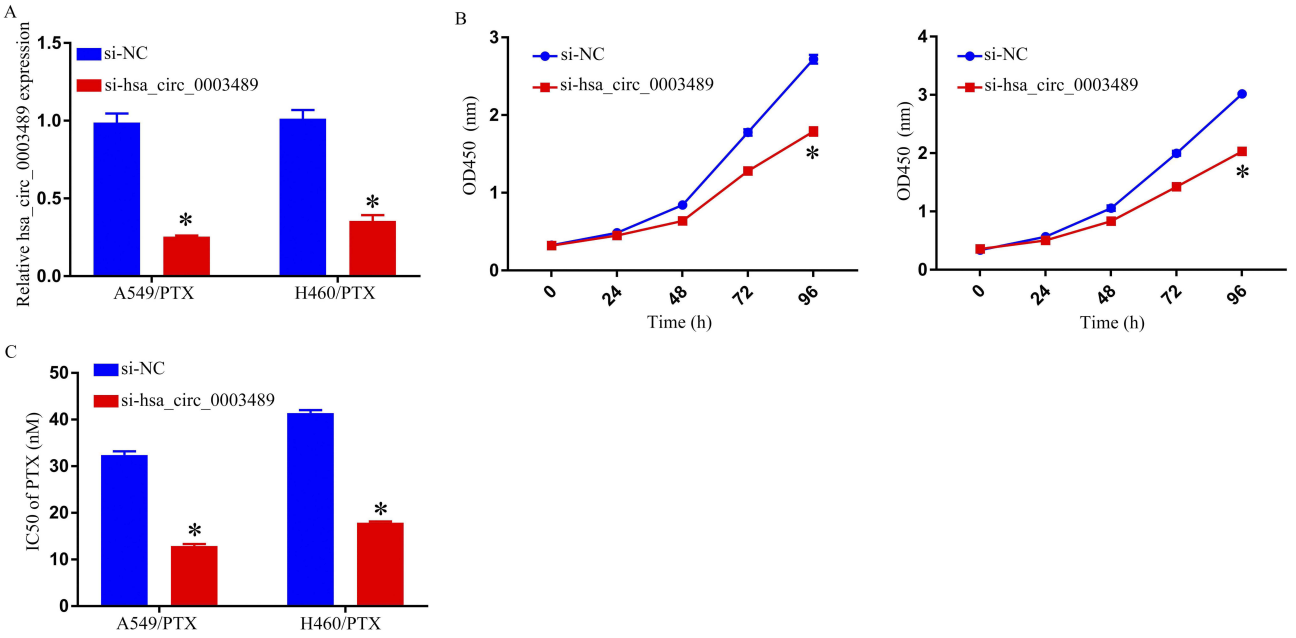

Figure 2 Suppression of PTX resistance in PTX-resistant NSCLC cells hsa_circ_0003489 knockdown. (**A**) qRT-PCR assay for hsa_circ_0003489 expression in A549/PTX and H460/PTX cells transfected with si-NC or si-hsa_circ_0003489. (**B**) Cell growth was detected by MTT assay. (**C**) MTT assay to determine IC50 of PTX in A549/PTX and H460/PTX cells. *p < 0.05.

miR-98-5p and IGF2-wt co-transfected 293T cells, but no difference was seen in IGF2-MUT groups (Figure 4B). Then, in order to investigate mechanisms for miR-98-5p influence upon GF2 expression, we transfected either miR-98-5p, anti-miR-98-5p, or respective controls. MiR-98-5p and anti-miR-98-5p were transfected into H460/PTX and A549/PTX cells, as shown in Figure 4C and D. We discovered that anti-miR-98-5p had opposing influence from those of miR-98-5p overexpression in terms of reducing the IGF2 expression in H460/PTX and A549/PTX cells. Additionally, our findings demonstrated that A549 and H460 cells expressed less IGF2 than H460/PTX and A549/PTX cells (Figure 4E and F). Normal tissues, PS tumor tissues, and PR tumor tissues showed an increasing trend of IGF2 expression (Figure 4G). In PR NSCLC tissues, the level of IGF2 mRNA was discovered to be inversely linked with miR-98-5p expression using Spearman correlation coefficient analysis (Figure 4H). In conclusion, miR-98-5p directly influenced IGF2 expression negatively.

Repression of Cell Progression and Enhancement of PTX Sensitivity Through miR-98-5p Overexpression Targeting IGF2

miR-98-5p, miR-98-5p+IGF2, miR-NC, or miR-98-5p+pcDNA-transfected, H460/PTX and A549/PTX probed involvement of miR-98-5p and IGF2 within PTX resistance. MiR-98-5p transfection downregulated IGF2 within H460/PTX and A549/PTX cells, but IGF2 transfection countered these effects (Figure 5A and B). Through functional tests, the overexpression of miR-98-5p in the H460/PTX and A549/PTX cells was found to significantly suppress cell growth and decrease PTX resistance, while the increase in IGF2 successfully overrode the effects (Figure 5C and D).

Decreased IGF2 Expression Through miR-98-5p Sponging by Hsa_circ_0003489 Knockdown

In order to probe relations among hsa_circ_0003489, miR-98-5p, and IGF2, H460/PTX and A549/PTX cell transfection was performed with si-NC, si-hsa_circ_0003489, si-hsa_circ_0003489+anti-miR-NC, or si-hs_circ_0001869+anti-miR-miR-98-5p. As seen in Figure 6A and B, anti-miR-98-5p successfully restored the silencing effects of hsa_circ_0003489 that markedly downregulated IGF2 in H460/PTX and A549/PTX cells. In PR NSCLC tissues, hsa_circ_0003489 was discovered

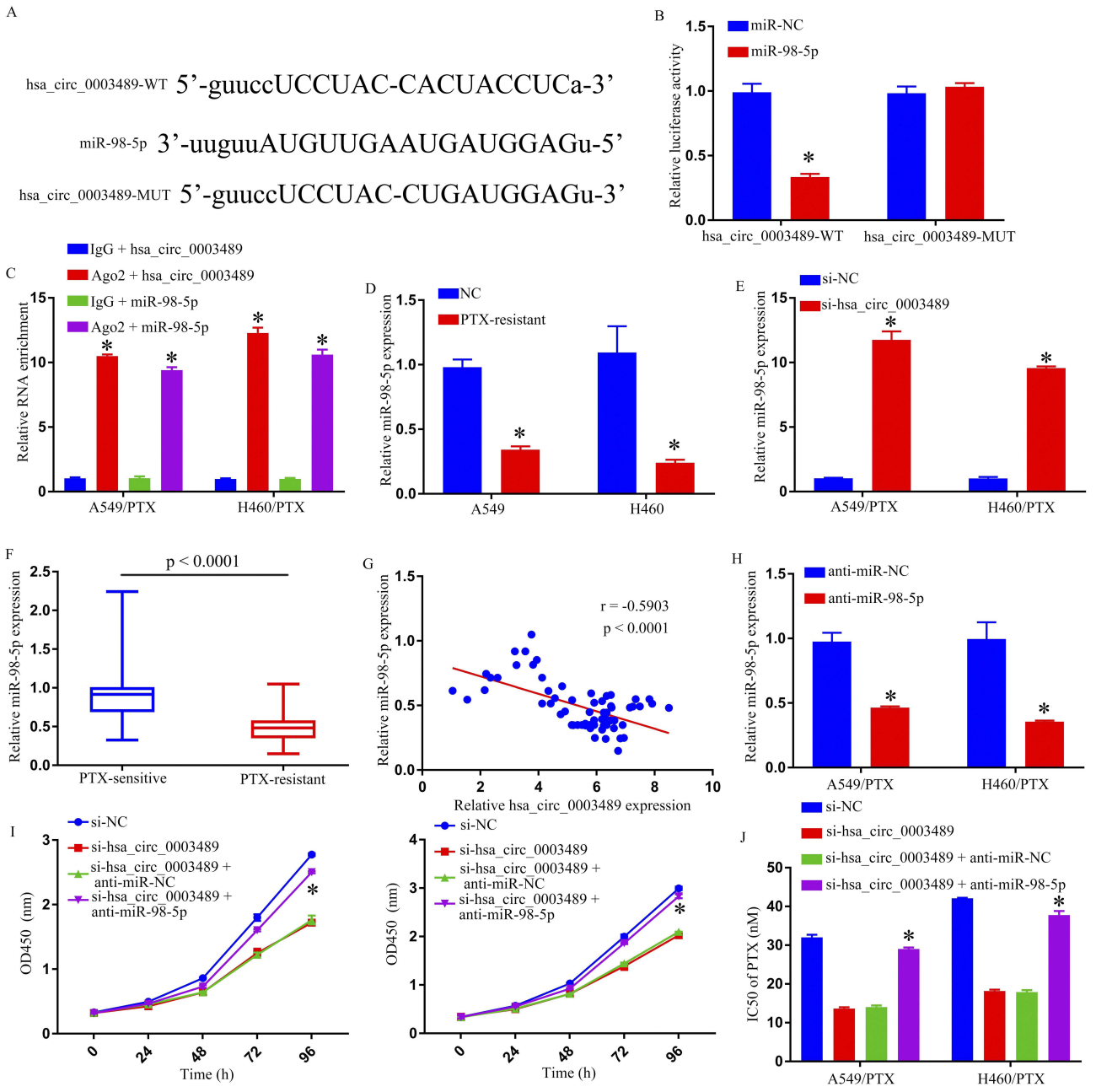

Figure 3 The hsa_circ_0003489 function as the sponge of miR-98-5p. (**A**) The potential binding sites between hsa_circ_0003489 and miR-98-5p. (**B**) The interaction between hsa_circ_0003489 and miR-98-5p in 293T cells was determined by dual-luciferase reporter assay. (**C**) RIP assay was performed to confirm whether hsa_circ_0003489 is bound to miR-98-5p. (**D**) QRT-PCR assay was used to determine the miR-98-5p level in A549, H460, A549/PTX, and H460/PTX cells. (**E**) The expression level of miR-98-5p in si-NC or si-hsa_circ_0003489 transfected A549/PTX and H460/PTX cells was examined by qRT-PCR analysis. (**F**) QRT-PCR assay was used for miR-98-5p level in PTX-sensitive and PTX-resistant NSCLC tissues. (**G**) The correlation between hsa_circ_0003489 and miR-98-5p in PTX-resistant tumor tissues was estimated by Spearman correlation coefficient analysis. (**H**) QRT-PCR assay was used to determine the miR-98-5p level in A549/PTX and H460/PTX cells transfected anti-miR-NC or anti-miR-98-5p. (**I**) Cell growth was detected by MTT assay. (**J**) IC50 of PTX was estimated by MTT assay. *p < 0.05.

to have a positive connection with IGF2 expression using Spearman correlation coefficient analysis (Figure 6C). Thus, we deduced that hsa_circ_0003489 favorably regulated IGF2 expression in PR NSCLC cells through miR-98-5p sponging.

Discussion

During clinical therapy, chemoresistance is a significant obstacle in treating human malignancies, particularly NSCLC. Recent developments in high throughput sequencing have pointed to various circRNAs as potential regulators of

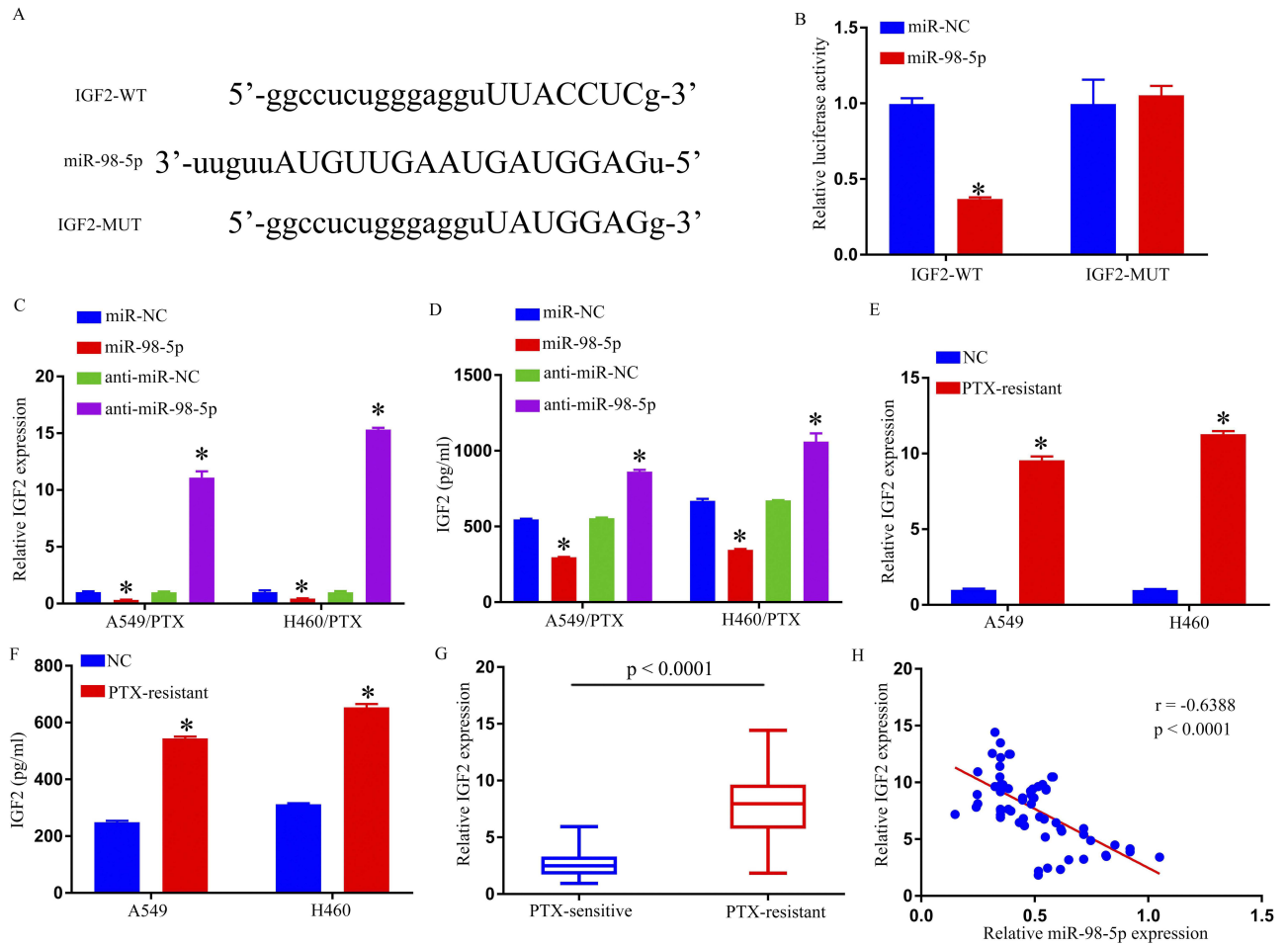

Figure 4 IGF2 was a direct target gene of miR-98-5p. (**A**) The predicted binding sites between IGF2 3′ UTR and miR-98-5p. (**B**) The interaction between IGF2 and miR-98-5p in 293T cells was determined by dual-luciferase reporter assay. (**C**–**F**) IGF2 expression was determined by qRT-PCR and ELISA. (**G**) QRT-PCR assay was used for IGF2 level in PTX-sensitive and PTX-resistant NSCLC tissues. (**H**) Spearman correlation coefficient analysis estimated the correlation between IGF2 and miR-98-5p in PTX-resistant tumor tissues. *p < 0.05.

chemoresistance. The current study focused on identifying the involvement of hsa_circ_0003489 in controlling NSCLC's PTX sensitivity. By controlling the miR-98-5p/IGF2 axis, hsa_circ_0003489 facilitated PTX resistance in PR NSCLC cells.

Researchers' interest has increasingly grown as they have learned more about the crucial functions that circRNAs play in NSCLC tumor development and drug resistance. For example, circ_0076305 controls cisplatin resistance in NSCLC by miR-296-5p sponging and regulating STAT3.[21] Depleting circ_0001821 inhibits the miR-526b-5p/GRK5 axis, which in turn reduces tumor growth, metastasis, and TAX resistance in NSCLC.[22] The miR-409-3p/TWIST1 axis is controlled by circ_0001658 in NSCLC to regulate resistance to gefitinib.[23] These results revealed that circRNAs performed distinct roles in the development of treatment resistance in NSCLC. As for hsa circ 0003489, it has been revealed that it promotes the progression of cancer.[19] High hsa_circ_0003489 levels were found in these tissues and cells of chemoresistant NSCLC. In vitro, PTX resistance in NSCLC cells was increased by hsa_circ_0003489 deficiency. hsa_circ_0003489 as a whole was involved in NSCLC's PTX resistance.

hsa_circ_0003489 was found to serve as the miR-98-5p sponge and then boost IGF2 expression during mechanism analysis. MiR-98-5p is said to target TGFBR1 and prevent NSCLC growth.[24] Targeting MAP4K3, miR-98-5p controls A549 cells proliferation and apoptosis.[25] Our findings here indicated that miR-98-5p levels were declining in NSCLC cells and tissues resistant to PTX. In PR NSCLC cells, miR-98-5p suppression could inverse influence from hsa_circ_0001869 knockdown on PTX sensitivity. Additionally, miR-326 overexpression increased PTX sensitivity in PR

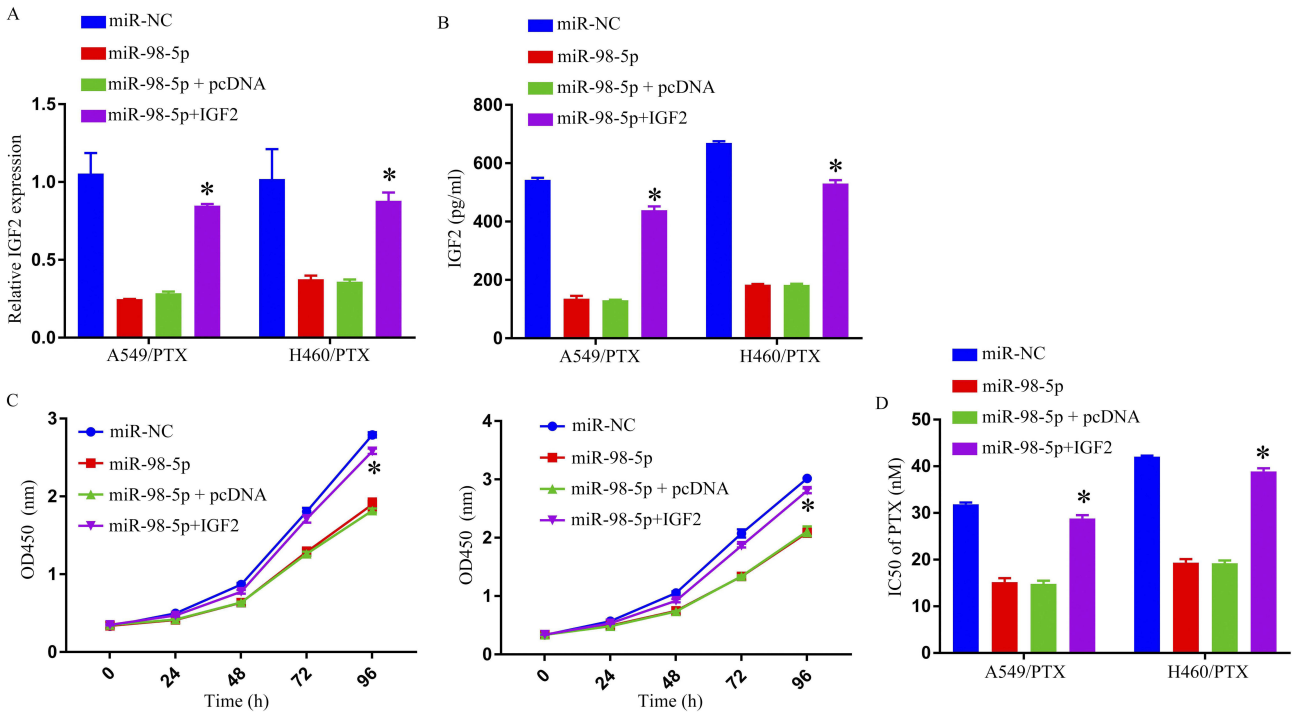

Figure 5 Overexpression of miR-98-5p enhanced PTX sensitivity and repressed cell progression in PTX-resistant NSCLC cells by targeting IGF2. (**A** and **B**) IGF2 expression was determined by qRT-PCR and ELISA. (**C**) Cell growth was detected by MTT assay. (**D**) IC50 of PTX was estimated by MTT assay. *p < 0.05.

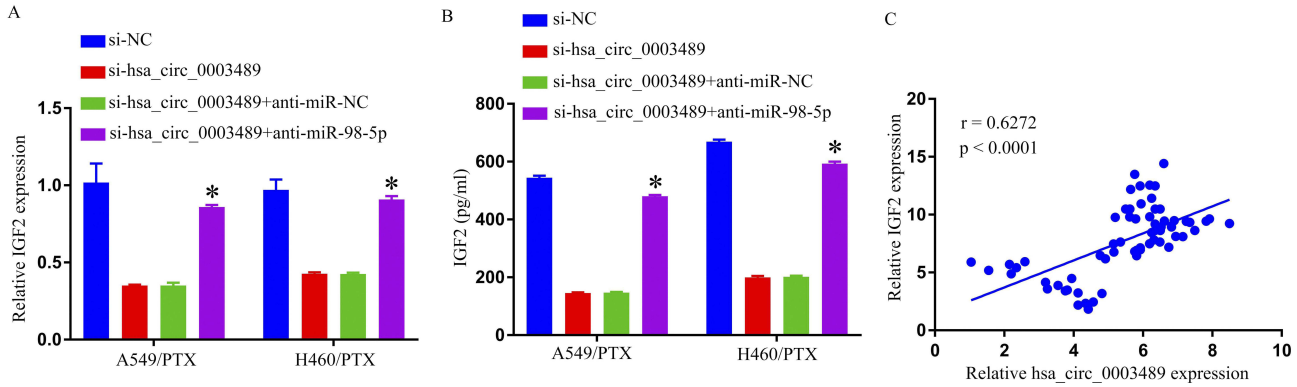

Figure 6 Hsa_circ_0003489 knockdown decreased IGF2 expression through sponging miR-98-5p. (**A** and **B**) IGF2 expression was determined by qRT-PCR and ELISA. (**C**) Spearman correlation coefficient analysis estimated the correlation between IGF2 and hsa_circ_0003489 in PTX-resistant tumor tissues. *p < 0.05.

cells, although these effects may be reversed by increasing IGF2. According to our findings, miR-98-5p inhibited PTX resistance in PR NSCLC cells by affecting IGF2. The assertion that miR-615-3p inhibits tumor metastasis and growth of NSCLC by inhibiting IGF2 is consistent with our findings and lends credence to this hypothesis.[26] In NSCLC, miR-647 increases cisplatin-induced cell apoptosis by inhibiting IGF2.[18] Notably, despite the fact that other miRNAs including miR-4521,[27] miR-185-5p,[28] and miR-138-5p[29] have been shown to target IGF2, we were the first to show an association across miR-98-5p and IGF2, pertaining to NSCLC chemoresistance. This study still has several shortcomings, though. For instance, we did not explicitly study the roles of IGF2 in NSCLC chemoresistance since the sample size was insufficient.

In conclusion, our results showed that has_circ_0003489 increased NSCLC's PTX resistance by modifying the miR-98-5p/IGF2 axis, signifying potential targets to overcome NSCLC's PTX resistance.

Disclosure

The authors reported no potential conflict of interest.

References

1. Bray F, Ferlay J, Soerjomataram I, Siegel RL, Torre LA, Jemal A. Global cancer statistics 2018: GLOBOCAN estimates of incidence and mortality worldwide for 36 cancers in 185 countries. *CA Cancer J Clin*. 2018;68(6):394–424. doi:10.3322/caac.21492
2. Barron-Barron F, Guzman-De Alba E, Alatorre-Alexander J, et al. National Clinical Practice Guidelines for the management of non-small cell lung cancer in early, locally advanced and metastatic stages. Extended version. *Salud Publica Mex*. 2019;61(3):359–414. doi:10.21149/9916
3. Cao M, Zhang L, Wang JH, et al. Identifying circRNA-associated-ceRNA networks in retinal neovascularization in mice. *Int J Med Sci*. 2019;16 (10):1356–1365. doi:10.7150/ijms.35149
4. Jiang C, Xu D, You Z, Xu K, Tian W. Dysregulated circRNAs and ceRNA network in esophageal squamous cell carcinoma. *Front Biosci*. 2019;24 (2):277–290. doi:10.2741/4717
5. Zhu J, Zhang X, Gao W, Hu H, Wang X, Hao D. lncRNA/circRNAmiRNAmRNA ceRNA network in lumbar intervertebral disc degeneration. *Mol Med Rep*. 2019;20(4):3160–3174. doi:10.3892/mmr.2019.10569
6. Hong W, Xue M, Jiang J, Zhang Y, Gao X. Circular RNA circ-CPA4/ let-7 miRNA/PD-L1 axis regulates cell growth, stemness, drug resistance and immune evasion in non-small cell lung cancer (NSCLC). *J Exp Clin Cancer Res*. 2020;39(1):149. doi:10.1186/s13046-020-01648-1
7. Zhang ZY, Gao XH, Ma MY, Zhao CL, Zhang YL, Guo SS. CircRNA_101237 promotes NSCLC progression via the miRNA-490-3p/MAPK1 axis. *Sci Rep*. 2020;10(1):9024. doi:10.1038/s41598-020-65920-2
8. Yang W, Wu L, Jin M. Hsa_circ_0041268 promotes NSCLC progress by sponging miR-214-5p/ROCK1. *J Clin Lab Anal*. 2022;36(4):e24262. doi:10.1002/jcla.24262
9. Du D, Cao X, Duan X, Zhang X. Blocking circ_0014130 suppressed drug resistance and malignant behaviors of docetaxel resistance-acquired NSCLC cells via regulating miR-545-3p-YAP1 axis. *Cytotechnology*. 2021;73(4):571–584. doi:10.1007/s10616-021-00478-z
10. Zhu K, Zhu J, Geng J, et al. circSNX6 (hsa_circ_0031608) enhances drug resistance of non-small cell lung cancer (NSCLC) via miR-137. *Biochem Biophys Res Commun*. 2021;567:79–85. doi:10.1016/j.bbrc.2021.06.032
11. Chen H, Li F, Xue Q. Circ-CUL2/microRNA-888-5p/RB1CC1 axis participates in cisplatin resistance in NSCLC via repressing cell advancement. *Bioengineered*. 2022;13(2):2828–2840. doi:10.1080/21655979.2021.2024395
12. Liu T, Song Z, Gai Y. Circular RNA circ_0001649 acts as a prognostic biomarker and inhibits NSCLC progression via sponging miR-331-3p and miR-338-5p. *Biochem Biophys Res Commun*. 2018;503(3):1503–1509. doi:10.1016/j.bbrc.2018.07.070
13. Shi Q, Ji T, Ma Z, Tan Q, Liang J. Serum exosomes-based biomarker circ_0008928 regulates cisplatin sensitivity, tumor progression, and glycolysis metabolism by miR-488/HK2 axis in cisplatin-resistant nonsmall cell lung carcinoma. *Cancer Biother Radiopharm*. 2021. doi:10.1089/cbr.2020.4490
14. Livingstone C. IGF2 and cancer. *Endocr Relat Cancer*. 2013;20(6):R321–R339. doi:10.1530/ERC-13-0231
15. Kasprzak A, Adamek A. Insulin-Like Growth Factor 2 (IGF2) signaling in colorectal cancer-from basic research to potential clinical applications. *Int J Mol Sci*. 2019;20(19):4915. doi:10.3390/ijms20194915
16. Luo L, Zhang Z, Qiu N, et al. Disruption of FOXO3a-miRNA feedback inhibition of IGF2/IGF-1R/IRS1 signaling confers Herceptin resistance in HER2-positive breast cancer. *Nat Commun*. 2021;12(1):2699. doi:10.1038/s41467-021-23052-9
17. Porras-Quesada P, Gonzalez-Cabezuelo JM, Sanchez-Conde V, et al. Role of IGF2 in the study of development and evolution of prostate cancer. *Front Genet*. 2021;12:740641. doi:10.3389/fgene.2021.740641
18. Jiang W, Zhao X, Yang W. MiR-647 promotes cisplatin-induced cell apoptosis via downregulating IGF2 in non-small cell lung cancer. *Minerva Med*. 2021;112(2):312–313. doi:10.23736/S0026-4806.19.06240-2
19. Tian FQ, Chen ZR, Zhu W, et al. Inhibition of hsa_circ_0003489 shifts balance from autophagy to apoptosis and sensitizes multiple myeloma cells to bortezomib via miR-874-3p/HDAC1 axis. *J Gene Med*. 2021;23(9):e3329. doi:10.1002/jgm.3329
20. Zhan P, Shu X, Chen M, et al. miR-98-5p inhibits gastric cancer cell stemness and chemoresistance by targeting branched-chain aminotransferases 1. *Life Sci*. 2021;276:119405. doi:10.1016/j.lfs.2021.119405
21. Dong Y, Xu T, Zhong S, et al. Circ_0076305 regulates cisplatin resistance of non-small cell lung cancer via positively modulating STAT3 by sponging miR-296-5p. *Life Sci*. 2019;239:116984. doi:10.1016/j.lfs.2019.116984
22. Liu Y, Li C, Liu H, Wang J. Circ_0001821 knockdown suppresses growth, metastasis, and TAX resistance of non-small-cell lung cancer cells by regulating the miR-526b-5p/GRK5 axis. *Pharmacol Res Perspect*. 2021;9(4):e00812. doi:10.1002/prp2.812
23. Yu X, Fu X, Zhang X, Bai C, Wang Y. Circ_0001658 regulates gefitinib resistance of non-small cell lung cancer through miR-409-3p/TWIST1 axis. *Anticancer Drugs*. 2022;33(2):158–166. doi:10.1097/CAD.0000000000001257
24. Jiang F, Yu Q, Chu Y, et al. MicroRNA-98-5p inhibits proliferation and metastasis in non-small cell lung cancer by targeting TGFBR1. *Int J Oncol*. 2019;54(1):128–138. doi:10.3892/ijo.2018.4610
25. Wang Z, Han Z, Zhang L, Zhang S, Wang B. MicroRNA-98-5p regulates the proliferation and apoptosis of A549 cells by targeting MAP4K3. *Oncol Lett*. 2019;18(4):4288–4293. doi:10.3892/ol.2019.10771
26. Su Y, Xu C, Liu Y, Hu Y, Wu H. Circular RNA hsa_circ_0001649 inhibits hepatocellular carcinoma progression via multiple miRNAs sponge. *Aging*. 2019;11(10):3362–3375. doi:10.18632/aging.101988
27. Xing S, Tian Z, Zheng W, et al. Hypoxia downregulated miR-4521 suppresses gastric carcinoma progression through regulation of IGF2 and FOXM1. *Mol Cancer*. 2021;20(1):9. doi:10.1186/s12943-020-01295-2
28. Zhuang ST, Cai YJ, Liu HP, Qin Y, Wen JF. LncRNA NEAT1/miR-185-5p/IGF2 axis regulates the invasion and migration of colon cancer. *Mol Genet Genomic Med*. 2020;8(4):e1125. doi:10.1002/mgg3.1125
29. Xue L, Tao Y, Yuan Y, Qu W, Wang W. Curcumin suppresses renal carcinoma tumorigenesis by regulating circ-FNDC3B/miR-138-5p/IGF2 axis. *Anticancer Drugs*. 2021;32(7):734–744. doi:10.1097/CAD.0000000000001063